2013 SCEC Annual Report

Modeling Slip Per Event on the San Andreas Fault from Fold Deformation Across a Step-Over at the Frazier Mountain Site

Ray Weldon – University of Oregon

Ashley Streig – University of Oregon

Kate Scharer – USGS

Summary of Major Research Findings

This report presents the first attempt to combine earthquake chronology and slip per-event estimates by evaluating structural relationships across a step-over at the Frazier Mountain paleoseismic site on the Southern San Andreas Fault (SAF). Transtensive step-overs, known as sags, are ubiquitous features of strike slip faults. At the Frazier Mountain site, the main trace of the southern San Andreas Fault steps to the right 40 m over 150 m along strike. Within the step are two adjoining synclines ~30 m x 70 m and ~10 m x 40 m in size. 34 paleoseismic trenches and 35 cone penetrometer tests spanning the step-overs show stratigraphic and structural relationships that demonstrate incremental coseismic fold and fault deformation. Rapid sedimentation generally buries the sag produced in an earthquake flattening the ground surface before the subsequent event. We quantify structural relief in individual ruptures across the step-overs using surveyed 3D point data for five key stratigraphic surfaces. 3D analysis suggests that three of four prehistoric events are similar in size to event FM1, the 1857 M 7.9 earthquake. Event FM4 is difficult to separate from the stratigraphic proximal FM5 but appears to be smaller than average. FM5 is slightly larger than other earthquakes, but is within typical along strike variability of displacement for surface rupture, or there is a previously unrecognized event between FM5 and 6 that is only recorded by folding in the investigation area excavated to date. Offset channels near the site suggest the 1857 earthquake (event FM1) generated ~5 m of lateral slip, and we document ~ 0.8 m of folding across the larger sag. We use the relationship between lateral slip on the fault and incremental sag deformation and find that 4 of the last 5 events produced ~ 4 – 5 m of lateral slip at the site.

Summary of Outreach Activities

Training and research experience for graduate student, Ashley Streig

Training and research experience for undergraduates; Rachel Lippoldt, Adam Arce, Andy Jerrett, Tracy Terrall, Nyle Weldon.

Introduction

Step-overs, or sags are often closed depressions frequently seasonally inundated, have abundant datable material (i.e. peats and charcoal), and high sedimentation rates, because of this sags are the best sites for preserving evidence of earthquake timing. It is clear from historical ruptures that these depressions grow incrementally during earthquakes (Guo et al., 2012). Our site is located on a releasing (right) step on the SAF, 40 m wide and 150 m long along strike (Figure 1). The goal of this study is to isolate vertical relief generated by prehistoric surface rupturing earthquakes across the step-over at the Frazier Mountain site (FM site), and use structural relief as a proxy for lateral slip on the fault. We carefully document and separate individual folding events and compare vertical relief generated across the site in the last five earthquakes. Geomorphic offsets measured both in the field and from LiDAR data near the site reveal 4 to 5 m of lateral displacement in 1857, FM1 (Sieh, 1978; Zilke et al., 2012; Madden et al., 2013), we compare the structural relief generated by this known range of slip in 1857 with structural contour maps of vertical relief for four earlier earthquakes, FM 2 - 5. Paleoseismic results of earthquake evidence and timing of these events at the FM site are presented in Scharer et al. (2014a, 2014b, 2015), and are only summarized here.

This study integrates trenching (including digitizing photomosaic trench logs), surveying, B4 LiDAR data, cone penetrometer testing (CPT) and GIS techniques to generate detailed 3D maps of subsurface geologic units, fault traces and related folds across the site (Figure 2). The goal of this analysis is to isolate vertical deformation step-wise, as close to the earthquake horizon as possible, for the last five earthquakes. This allows us to directly compare the fold orientation, geometry and vertical relief of deformation generated by each earthquake. The general process, assumptions and complications to retrodeforming these stratigraphic horizons are described in detail in Streig, 2014.

Frazier Mountain Site

The FM site is located in a 100 x 500 m closed depression on a releasing step on the northwest end of the Mojave section of the San Andreas Fault (SAF) (Figure 1). The margins of the depression are formed by prominent scarps on the northeast and southwest, and trenching reveals that these scarps are associated with older fault traces that do not offset deposits in the age range considered here (Figure 2). Faulting along the prominent northeast scarp (Figure 1b, yellow dashed lines) occurred more than 1,200 years ago (constrained by trenches across the older boundary on both sides of the depression, Figure 2), and since then slip has been concentrated across a narrower step in the fault. Younger cross-basin faults have formed within this narrow step and offset historic deposits, our network of trenches and CPT's are concentrated in this area (Figure 2). Stratigraphy at the site is generally fine-grained, and

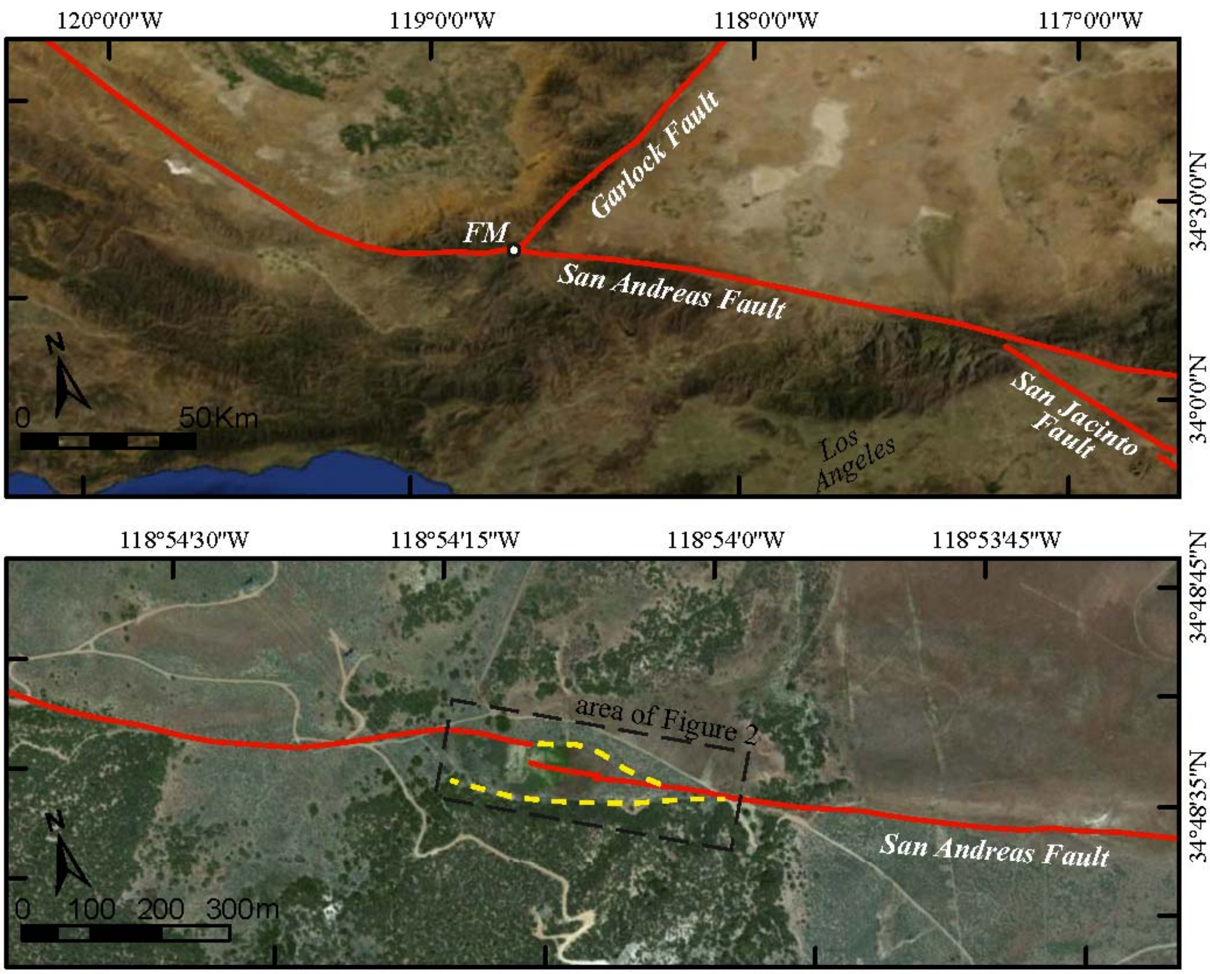

Figure 1. (a) Satellite image of the 'Big-Bend' region of the Southern SAF, CA, the Frazier Mountain site shown as FM (NASA Blue Marble: Next Generation imagery, Source: ESRI). Major faults are shown as red lines. (b) The 100 x 500 meter closed depression (shown in yellow where faults are no longer active) formed in a stretch of the fault where the surface traces of the SAF diverge in a transtensive manner from the regional trend. The past 5 – 10 earthquakes have bypassed the eastern edge of the older, larger step and appear to be the beginning of the end of the step-over. Aerial imagery of the Frazier Mountain paleoseismic site (i-cubed Nationwide Prime, Source ESRI).

dominated by alternating silt to organic-rich mud deposits interbedded with broadly tabular, massive, well-sorted, fine-grained sand layers (Figure 3, 4). These sand layers are laterally continuous and distinctive enough to confidently trace through the site. There is an abrupt transition to poorly sorted, gravelly sand capping the site in the last ~200 years (Figure 4).

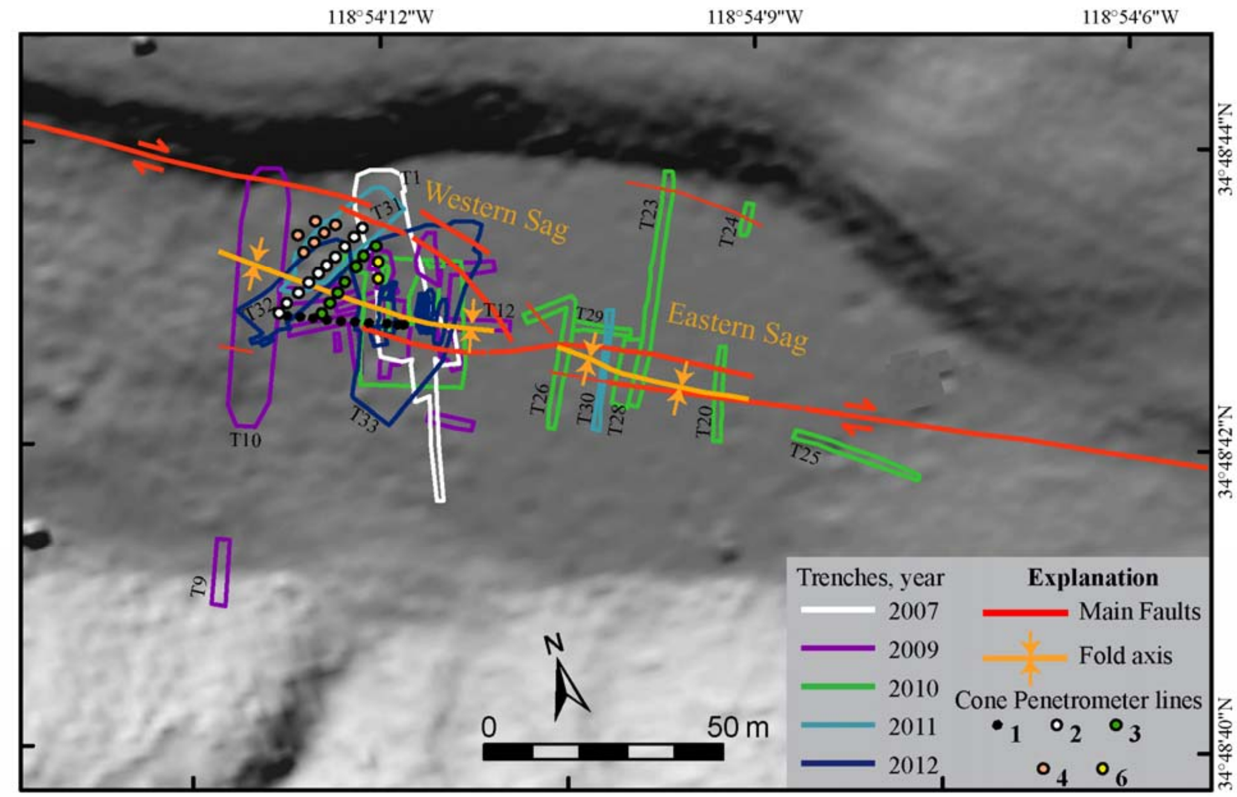

Figure 2. Frazier Mountain site map showing locations of trenches excavated in 2008, 2009, 2010, 2011 and 2012, and Cone Penetrometer (CPT) transects (2011, before the 2011 and 2012 trenches) in the northwestern portion of the site. Major, faults and syncline axes associated with the past 6 earthquakes are constrained by trench exposures of the structures and are shown as red and orange lines on the map, respectively. Hillshade derived from B4 lidar data (downloaded from OpenTopography).

Methods

Paleoseismology and Surveying

We excavated 34 trenches, a combination of vertical slot trenches in the upper 2 - 3 meters, and 'V' trenches with ~ 30° sloped walls from the surface or below 'boxes' cut into the previously trenched upper 2 – 3 meters in 2007, 2009, 2010, 2011, and 2012 (Figure 2). Trench exposures were cleaned, and gridded with a string and nail grid, and photographed. Grids in slotted trenches on vertical benches were 1 m x 0.5 m (horizontal x vertical), and larger 'V' trenches were gridded with 1 m x 0.65 or 1.3 m grids (horizontal x face perpendicular; Figure 3) to account for the slope of the trench wall; this allows us to plot photomosiac logs to a 1 x 0.5 or

1m grid when projected onto a vertical plane. All trench exposures were logged on a printed photo mosaic of high-resolution digital photographs at a scale of roughly 1:10. Stratigraphic units and structural relationships were documented and described on photo logs.

We surveyed trench edges, trench grids, the base of every unit that was thick enough or laterally extensive enough to correlate between trenches, faults, fissures and other ground shaking related features exposed in each trench, and surveyed or hand measured small cut-backs into primary trench walls during each field season. We used a Leica total station, and installed a network of benchmarks the first and second years of the study to place all surveys in a common reference frame, and merge data sets for five investigation years. Horizontal uncertainties between survey years are less than 5 cm for surveys in 2010, 2011 and 2012, with horizontal errors less than ~10 cm for surveys in the years 2007 and 2009. We surveyed the benchmarks and some trench locations with a differential GPS unit (Trimble GeoXH), and used these coordinates to translate and rotate total station survey data in a Cartesian coordinate system to WGS 84 UTM zone 11N projection. GPS positions were post processed using Trimble Pathfinder software and a network of permanent GPS base stations to reduce position uncertainty.

Cone Penetrometer Test transects (CPT)

We used Cone Penetrometer Tests (CPT) transects to laterally extend observations of key stratigraphic units identified in the upper ~8 meters of section in excavations, and to see how deformation changed with depth below our excavations. CPT's were carried out by Gregg Drilling and Testing, Inc. using a 25-ton CPT rig with a 15 cm^2 piezocone (cone number GDC-36), and data was recorded at 5 cm intervals down to about 20 meters on average. The data were collected on August 15 – 16, 2011, and named "FRAZIER MOUNTAIN SITE – Job 600". Raw data and calibration specifics are available from Gregg Drilling or the authors of this interpretation . The CPT rig recorded; Depth, Tip Pressure, Sleeve Pressure, Pore Fluid Pressure, Tilt X, Tilt Y, UVIF (Ultraviolet Induced Fluorescence), Resistivity, and Temperature. CPT locations are shown in Figure 2, additional details on processing and interpreting these data are available in Streig, 2014.

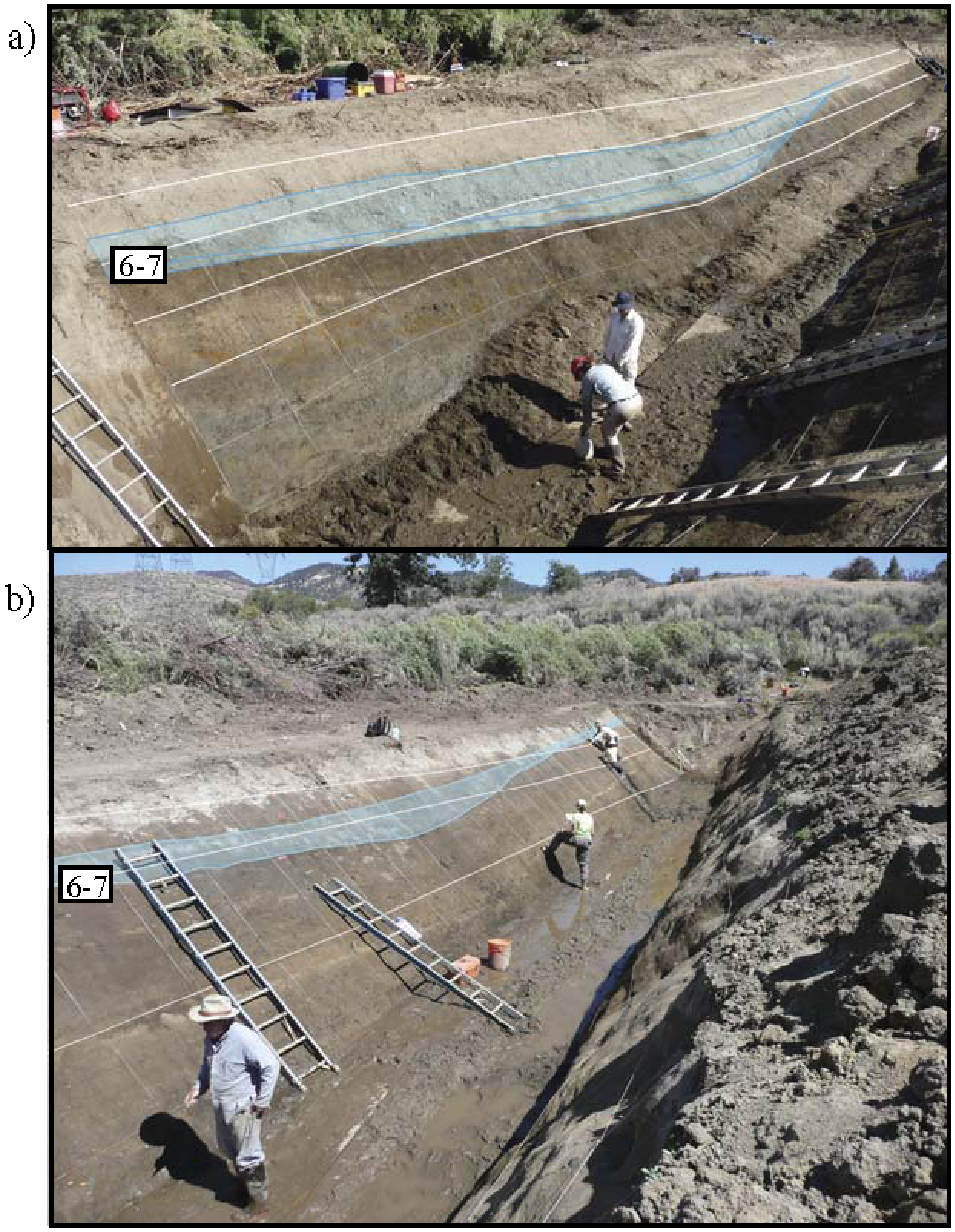

Figure 3. Photographs highlighting fold deformation. Units 5-7 are colored so the lower surface is the base of unit 7 and the upper surface is the base of unit 4 a course sand to gravel, shown as a blue polygon in both photos. (a) Photograph of trench T10 West wall, and (b) Trench T1 West wall, cut1. The base of unit 7 drops about ~1 meter from the outer edges of the fold limbs to the fold axis. Units 5-7 thickens in the fold axis, and are twice as thick in center of fold as the limbs of the fold. The top of the blue polygon is the base of Unit 4, folded in FM1. The base of the blue polygon, unit 7,is folded in two events, FM1 and FM2. Units 5-7 are thicker in T10 (a), the westernmost trench, which is closer to the sediment source than all other trenches. T1 (b) is ~15 m east of T10, and units 5-7 are noticeably thinner. [Note: The apparent warping of the white grid in the upper photos (T10E) is due to an irregular wall and the perspective of the photo; the grid is really horizontal and spaced 50 cm apart vertically.]

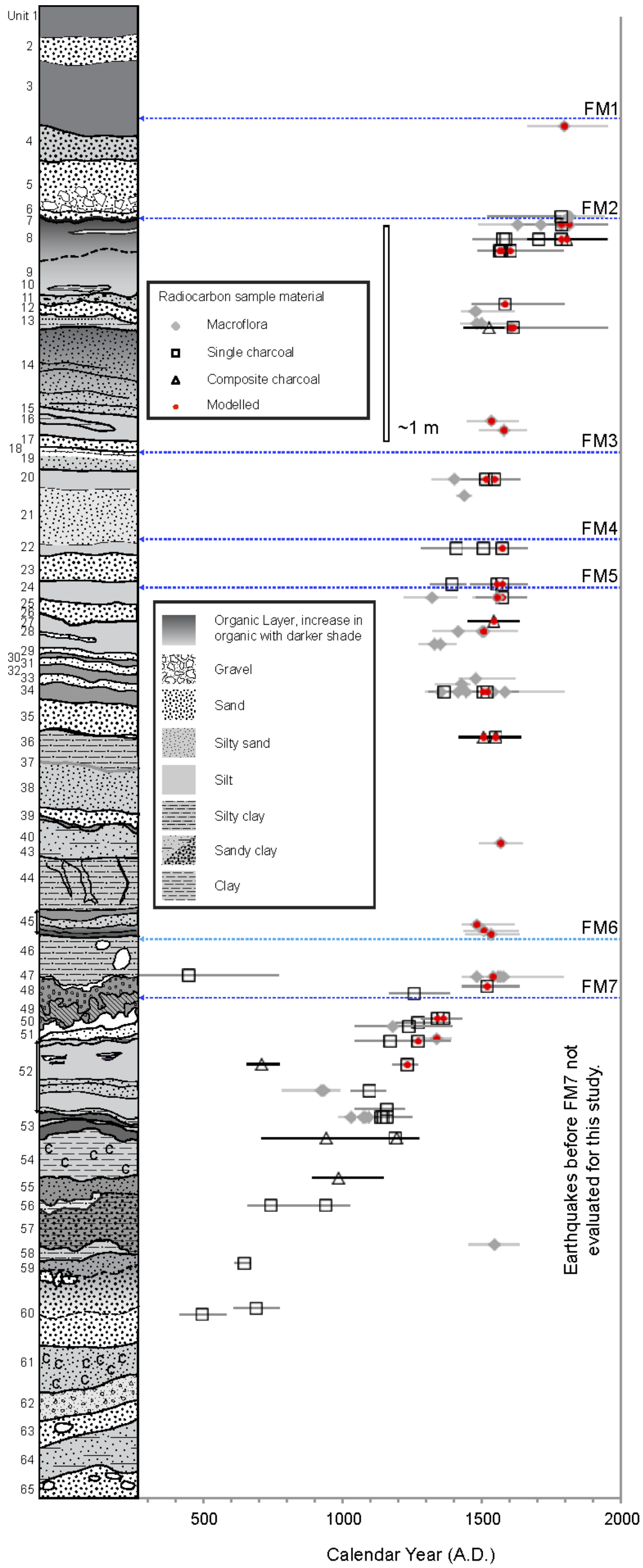

Figure 4. Stratigraphic column showing deposits, relative locations of dated radiocarbon samples and earthquake horizons at the Frazier Mountain site. Key to stratigraphic patterns, and explanation of radiocarbon sample material (i.e. charcoal, macrofossil etc.) shown on the right. Samples shown with red centers were stratigraphically consistent and retained in the site's age model (Dating results and the final OxCal model are included in Scharer et al., 2014a, b).

Summary of Earthquakes at Frazier

The oldest earthquake structure contoured in this study, FM 5, generates folding in both the Eastern and Western Sags for deep stratigraphic units, 25 to 35 (Figure 5, 6). This event occurred while unit 24 was at the ground surface and has upward fault terminations extending into units 24 and 25. Units 23 and one lower unnumbered unit are growth strata that on-lap and partially infill vertical relief across faults and sagging generated in this earthquake (Figure 5). FM5 has an OxCal modeled 2σ age range of 1510 to 1572 (Scharer et al., 2014).

Earthquake FM4 offsets the base of unit 22 and unit 23, a well sorted sand, ~10 cm across a fault that trends roughly N50W through the center of the Western Sag, and documented in trenches T1 and T31 (Figure 6, 7). Unit 23 records all deformation in FM4, and because it is the upper portion of a sequence of growth strata deposited after the previous event (FM5) it also records some part of FM5 deformation. Vertical relief generated by the FM4 earthquake is largely infilled by unit 21 (observed in T1, unit not identified in T31). FM4 yielded a 2σ age range of 1540 to 1606 (Scharer et al., 2014a, b). Unit 21 is not traceable through the site, so we chose to structure contour the more laterally continuous unit 23 to best approximate FM4 deformation.

Earthquake FM3 is distinct in both the Eastern and Western Sag, this earthquake generated small cracks and fissures on the order of a few centimeters wide and tens of centimeters deep in unit 18, and extending downward into units 19 and 20 (Figure 4). Unit 18, a thin finely laminated clay bed, was at the ground surface at the time of FM3, and fissures and relief generated by this earthquake were subsequently filled with sand of unit 17 (Figure 4, 5, 6). A few faults exhibit vertical separation in FM3, but most vertical relief at this horizon is accommodated by fold deformation. FM3 has an OxCal modeled 2σ age range of A.D. 1563 to 1626. Units 5, 6 and 7 post-date earthquake FM2, and together are twice as thick in the center of the fold as in the limbs (Figure 3, 5). Units 6 and 7 are sand (6) and discontinuous 1-2 cm thick organic stringer (7), where it is present at the base of unit 6. Units 6-7 are the basal, fine-grained facies of a thick poorly sorted gravelly sand, units 5 and 6 (Figure 3). FM2 caused significant folding, and units 5 and 6 filled the depression generated by this event. FM2 has a 2σ OxCal modeled age range of 1733 – 1854, and could be the historic 1812 earthquake. FM 1 postdates unit 4, a silty sand, and occurred within unit 3, an organic silt. Silt and sand deposits, units 1 and 2, overlie unit 3 and are not involved in any earthquakes (Figure 4). FM1 is the historic 1857 M7.9 SAF earthquake that extended from Parkfield at the north (the northern end of Figure 1), south to the junction with the San Jacinto Fault (Figure 1).

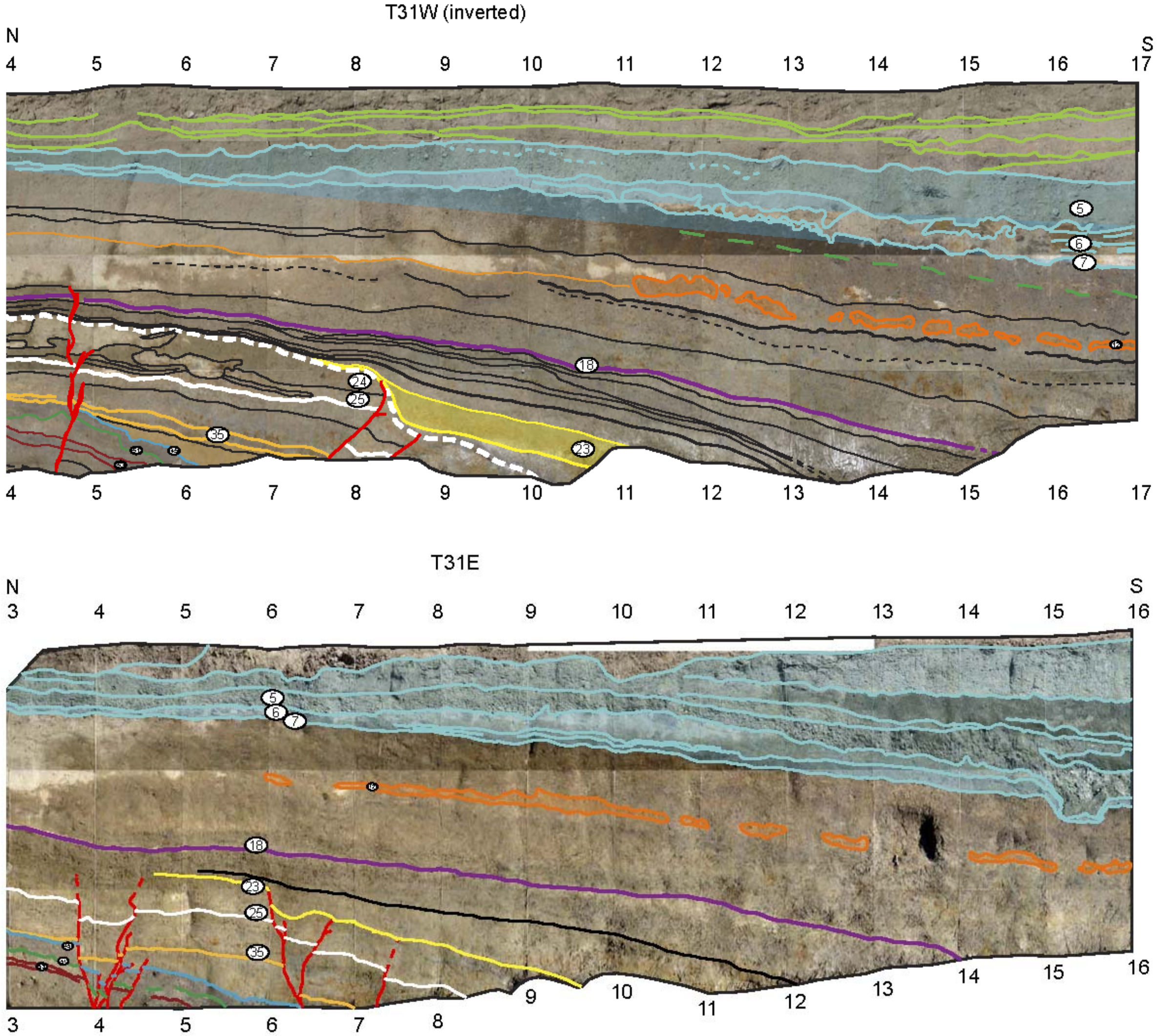

Figure 5. Photomosaiced trench logs from the Western Sag, for trench (a) T31W (west wall, inverted), and (b) T31E (east wall). Stratigraphic units are mapped as solid lines and shaded colored polygons. Sequences of sedimentation infilling relief from sag-deformation (folding) caused by earthquakes can be seen where units thicken from the northern margin of the step-over toward the south. Broad ~40 m wide, fairly symmetrical fold deformation is observed in the Western sag. (a) Trench T31W, the FM5 earthquake horizon is shown as a white dashed line below unit 23. Unit 23 is part of the growth strata sequence infilling vertical relief generated in earthquake FM5, and has infilled only ~ 1/3 to 1/2 the structural relief created by rupture across the step-over in that event. The base of unit 23 is lithologically distinct, and is laterally extensive between trenches, and is the most continuous unit between earthquakes FM4 and FM5 and so was used for the FM4 earthquake fold surface.

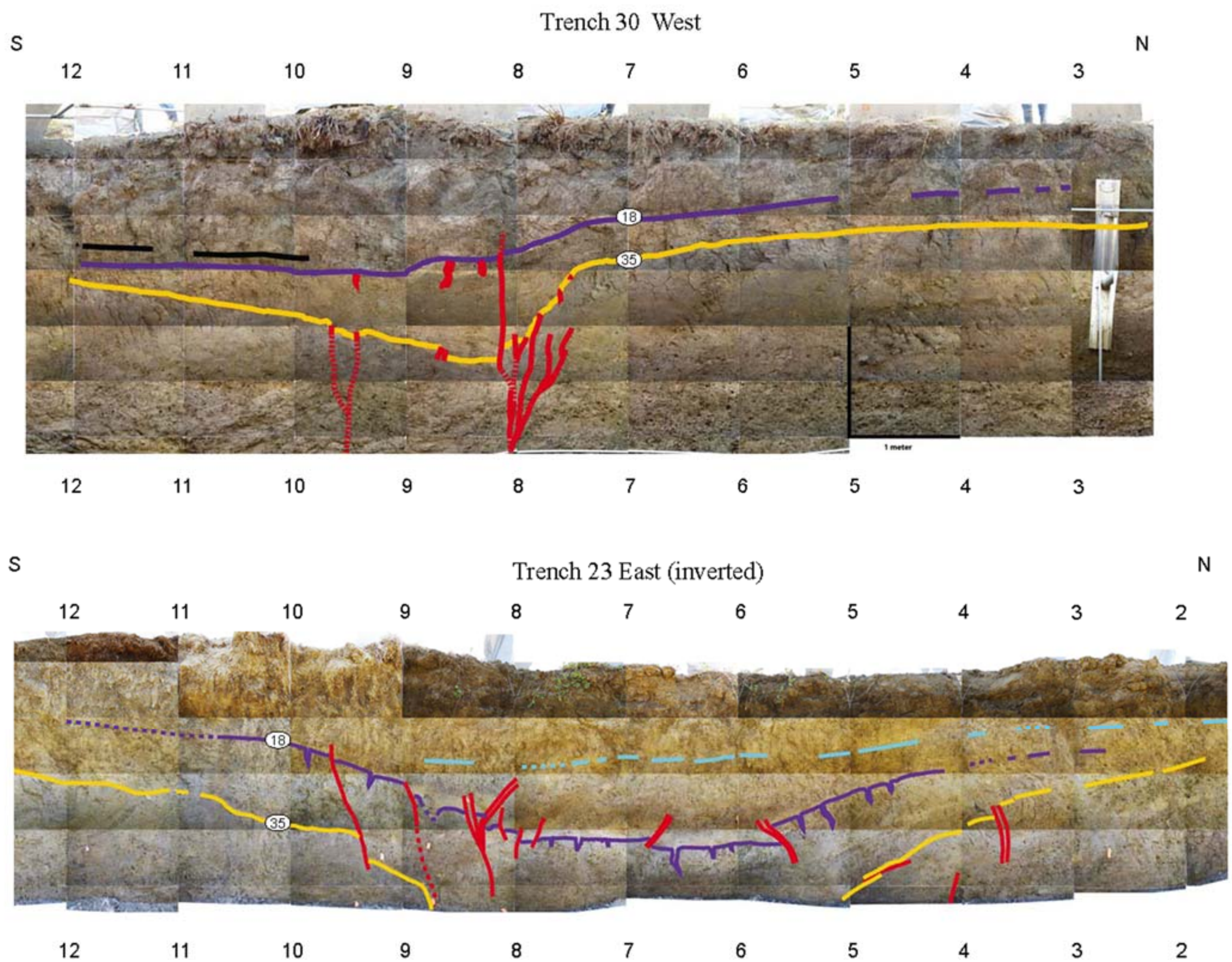

Figure 6. Photomosaiced trench logs from the smaller, Eastern Sag for trenches (a) T23 and (b) T30. Folding in the Eastern sag about 7 m wide, and asymmetrical across the synclinal fold axis to the east, shown in trench T23. Vertical relief is largely accommodated along the sag margins, the base of the sag is roughly flat bottomed to gently dipping.

Data Compilation

We generate structure contour surfaces for the base of units, 4, 6-7, 18, 23 and 35 to represent deformation in events FM1through FM5 respectively. We compile data for unit 35 for FM5 structure contouring because it is the most distinct and extensive stratigraphic unit between the FM4 and FM5 earthquake horizons, and was widely surveyed in the field. However, unit 35 is 10 stratigraphic units below the FM5 event horizon, the greatest stratigraphic distance from the earthquake surface of interest of all the units evaluated here. Unit 35 is high in the stratigraphic section above FM6, separated by 10 older stratigraphic units (units 45 to 36; Figure 4) that appear to completely infill structural relief generated by earthquake FM6. Future work will involve carefully measuring and compiling unit 25 from trench logs, to better bracket the FM5 event horizon. This unit is less distinct and was difficult to correlate between trenches while in the field, but should be possible if the unit was identified and logged in all exposures by comparing photomosaic logs and stratigraphic sections side by side. This additional step may help us more carefully separate deformation associated with FM5 from FM6, and test whether there is an additional event between FM5 and FM6.

Because stratigraphic units thin and taper out of the sags we locally employed a pinch out rule to extend observations of units based on the presence of their conformable basal contact with underlying stratigraphy. We used this rule where trench logs show stratigraphic relationships, but we lack survey data for a unit. The resulting 3D point data reflect observed tapering relationship of the deposits, and the margins of the deposits don't abruptly end. We also added zero values where units pinch out to place a hard sedimentary boundary on the sag-filling shape of the deposits. These steps minimize edge effects on interpolated surfaces and contours of the stratigraphic surface data. We added CPT inferred depths for units 6, 18, 23 and 35 to the compiled stratigraphic trench survey data.

Results

3D Structural Analysis

We plot elevations of the stratigraphic horizons to portray the density and areal data coverage for each surface (Figure 7). We interpolate a surface through these elevations; this surface reflects deformation for all earthquakes a unit has experienced and to varying extents unfilled deformation from the earthquake below. Stratigraphic survey points do not directly overlie each other, so, to retrodeform sag filling deposits, we must either subtract one surface from another, or subtract the points for a given event from a surface fit to another set of points.

The latter produces the least interpreted and most artifact-free results. We tried progressively retrodeforming interpolated surfaces earthquake by earthquake, but found small variations in each retrodeformation step compound, producing artifacts in multiply deformed surfaces. We difference the point data for each earthquake surface from an interpolated surface for the previous earthquake to isolate the folding for each earthquake horizon. For example, if we want to evaluate vertical relief generated in FM3 we difference the point data for unit 18 from the 'total deformation' surface for unit 7 that is deformed by earthquakes FM1 and 2, but is inferred to postdate complete infilling of relief generated by earthquake FM3. Differencing earthquake surfaces isolates folding in each event, and also largely removes the depositional gradient for these low energy distal alluvial deposits. This is because the deposits are lithologically similar, have the same alluvial sediment source on the western margin of the step-over, and the units are all generally fine-grained depression filling deposits, and so have similar trends and ranges of surface gradients. The differenced points have values ranging from 0 (i.e. no change) to negative values (reflecting downward change). Surfaces interpolated from these differenced points reflect sag deformation for FM1, FM2 and FM3 (Figure 7).

FM1, 2, 3 and 5 have 70, 83, 85 and 80 cm of structural relief across the sag respectively, and the values for FM5 are a minimum. FM4 has 47 cm vertical relief at its greatest depth, this is a maximum value of structural relief, since unit 23 also captures a fraction of FM5 deformation. A correction can be made between FM4 and FM5 estimates to better represent deformation in each of these earthquakes. We know from trench exposures that unit 23 infills roughly the upper 1/3 to 1/2 of relict relief from FM5 (Figure 5), so the maximum depth value of 47 cm of vertical relief in FM4 (Figure 7h) can be divided by 2 to yield ~ 24 cm of structural relief in FM4, and is a better estimate for this event. We can add the remaining 24 cm to the FM5 value of 80 cm of structural relief across the sag, totaling over 1 m of vertical relief in earthquake FM5. We can see in Figure 7h that structural relief for the uncorrected FM4 surface is not as pronounced, or sharp on the step-over margins as the other earthquake surfaces (Figure 7). Reducing vertical relief by half would make the FM4 surface even more gently folded, and strikingly dissimilar to the amount of vertical relief generated in the other four earthquakes.

Figure 7. (next page) Elevation of stratigraphic point data where warm colors are high elevations and blue are lower (left column) and retrodeformed surfaces (right column) for unit 4 (a)(b), unit 6-7 (c)(d), unit 18 (e)(f), unit 23 (g)(h) and unit 35 (i)(j). 1 m color ramp in the right column for all surfaces, where 0 m relief is shown as red and equals no change in surface position (elevation), and increased vertical sagging shown as increasingly cool colors, where 1 m+ of vertical deformation is shown as dark blue. Thin black lines on surfaces are 25 cm contours.

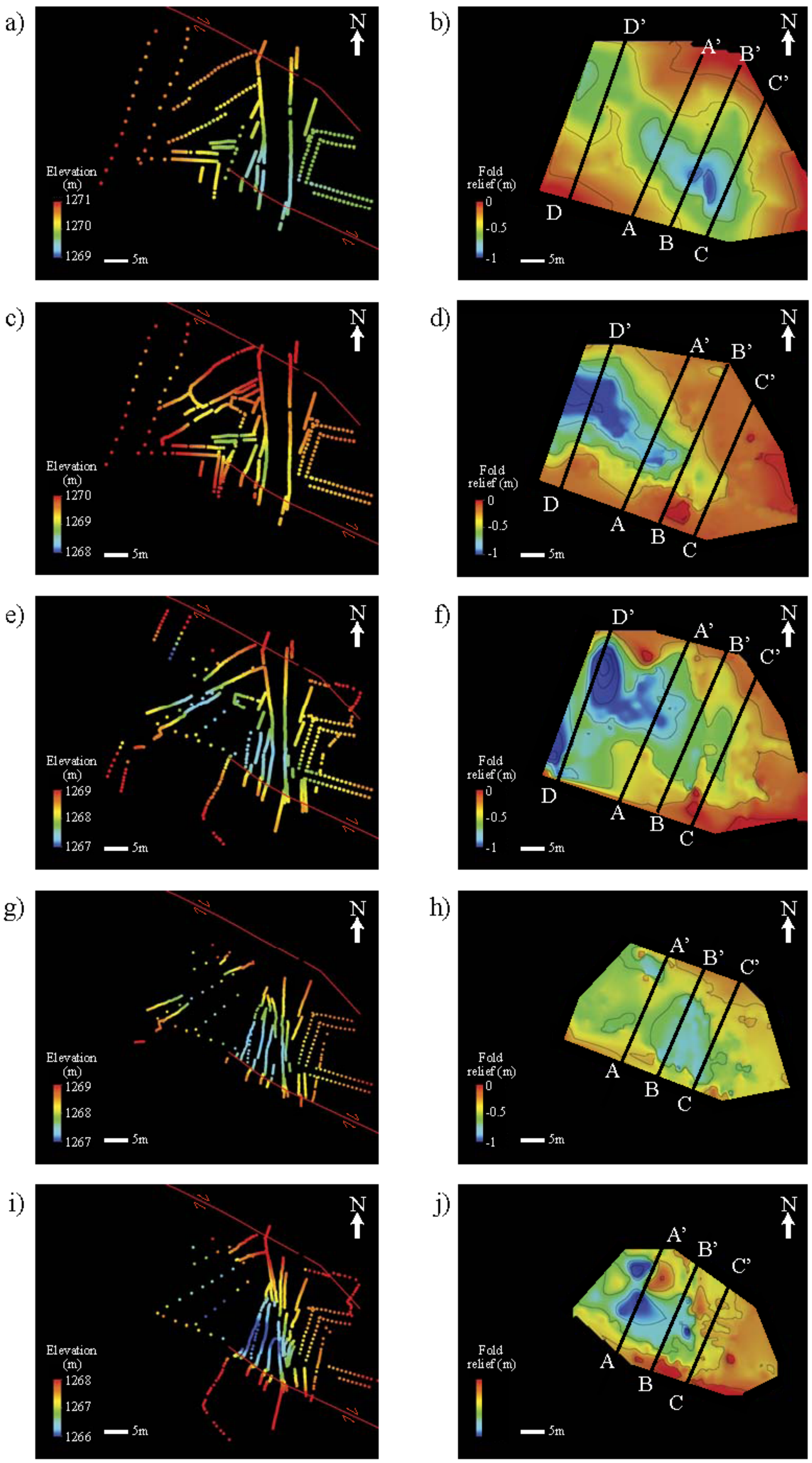
a)
N
Elevation (m)
1271
1270
1269
5m
b)
N
D'
A'
B'
C'
D
A
B
C
Fold relief (m)
0
-0.5
-1
5m
c)
N
Elevation (m)
1270
1269
1268
5m
d)
N
D'
A'
B'
C'
D
A
B
C
Fold relief (m)
0
-0.5
-1
5m
e)
N
Elevation (m)
1269
1268
1267
5m
f)
N
D'
A'
B'
C'
D
A
B
C
Fold relief (m)
0
-0.5
-1
5m
g)
N
Elevation (m)
1269
1268
1267
5m
h)
N
A'
B'
C'
A
B
C
Fold relief (m)
0
-0.5
-1
5m
i)
N
Elevation (m)
1268
1267
1266
5m
j)
N
A'
B'
C'
A
B
C
Fold relief (m)
5m

These surfaces show that, in general, in the area we have excavated, the northern margin of the syncline is less steep than the south margin. 25 cm interval surface contours show that elevations gradually rise over 10 to 15 m distance to the north edge of the step-over (Figure 7, and the floor of the syncline is roughly flat bottomed to gently dipping. Overall, we find that the shape of the syncline is strikingly similar for all five earthquake surfaces.

We compare the volume and area folded in each of the earthquakes by measuring volume of fold relief below the inflection from gradual to steep surface slope along the sag margins (Table 1; Figure 7). We know that most vertical relief is captured at the margins of the sags, so, the area below this inflection point should reflect most structural relief generated by each earthquake. The inflection point ranges from ~ -0.5 to -0.75 m of structural relief, shown by the color ramp for all surfaces in Figure 7 (approximately the yellow to orange transition). We measure fold volume below this inflection point on the basin margins for a swath of topography clipped between lines A-A' and C-C' shown on Figure 7. This area overlaps in all surface models, so we can directly compare structural relief generated event by event for exactly the same location. Using the entire surface model would bias fold relief volumes towards the higher stratigraphic units that have more areal coverage. However, the method used here still biases toward stratigraphically higher surfaces; lower surfaces for FM 4 and FM5 (Figure 7h, j) are shorter in the northeast – southwest direction (perpendicular to the fold axis). However, this should have a small effect in this comparison because the inflection for these surfaces is in-board (basin-ward) of the surface edges.

We consider fold volume to be a proxy for vertical relief over an area. We find that earthquake FM1 has greater fold volume than all other surfaces. FM2 and FM3 have roughly the same amount fold volume. FM3 is roughly 85% of FM2, but the greatest structural relief at the FM3 horizon occurs west of the area we analyzed (Figure 7f). FM4 has smaller fold volume than the other four earthquake surfaces and is an overestimate because this horizon includes some fraction of FM5 deformation. FM5 values are minimum estimates and should increase to values similar to FM2 and 3 (Table 1), with a correction for the relict FM5 relief included in FM4 estimates. Overall, structural contour maps and fold volume estimates highlight the similarities in sag (fold) geometry and orientation for all five events, and reveal similar structural relief in the Western Sag for four of the last 5 events.

Table 1. Volume and Folding estimates of vertical relief generated by earthquakes FM1 through FM5.

Earthquake	Fold Volume (m^3)	Fold Area (m^2)
FM1 (1857)	127	570
FM2	78	368
FM3	67	376
FM4	43	312
FM5	55	245

* Note the volume of unfolded unit 23 is not equivalent to FM4, so values here are high, and includes a fraction of FM5 deformation.

#FM5 values are low, some fraction included in FM4. With a correction FM5 values will increase, and FM4 will decrease.

Discussion

Retrodeformed stratigraphic surfaces allow direct comparison of fold shape, orientation, and amplitude for the last five earthquakes. We find that rupture across the step-over generated a long trough trending N55 – 60°W for earthquakes FM 1 through 5 (Figure 7). Retrodeformed and gradient corrected surfaces in Figure 7 have 25 cm contours to highlight narrow, steep areas with the greatest structural relief. This highlights that the majority of vertical relief generated in a rupture is concentrated on the margins of the sags and is accommodated by both oblique normal faulting and folding. These findings are also similar to experimental clay models for an oblique step-over (e.g. Mitra and Paul, 2011), and observations of ruptures across releasing step-overs in earthquakes (e.g. 2010 Yushu earthquake, China, Guo et al., 2012). From studies such as these we know the ratio of lateral slip outside the step-over and vertical relief within the step-over vary based on step-over geometry, size, and depth of the step.

We know 4 - 5 m of slip occurred across the active, 40 m wide, 150 m long step-over at the site in 1857, FM1 (Sieh, 1978; Madden et al., 2013); and so at least 2 earlier earthquakes must have had similar slips. One earlier earthquake, FM4, is smaller than all the others, probably generating~ 0.24 m of structural relief, sagging, across the step-over. The earliest earthquake considered here, FM5 generated 1/3 more structural relief across the step-over than 1857, and so must have had larger slips at the site. We conclude that earthquakes FM1, FM2 and FM3 are very similar and slip in FM5 is only ~ 33% greater, and within a 0.6 coefficient of variation, which is the variability of surface displacement at a point on a fault (Hecker et al., 2013). Earthquake FM4 has smaller displacement than the other five earthquakes, and is not within the coefficient of variation of 0.6 for the FM1 vertical displacement, and so must represent smaller slip at the site in that earthquake.

References Cited

Guo, J., Zheng, J., Guan, B., Fu, B., Shi, P., Du, J., Xie, C., Liu, L., 2012. Coseismic Surface Rupture Structures Associated with 2010 Ms 7.1 Yushu Earthquake, China. Seismological Research Letters, 83, 109-118, doi:10.1785/gssrl.83.1.109.

Hecker, S.A., Abrahamson, N.A., Woodedell, K.E., 2013. Variability of Displacement at a Point: Implications for Earthquake-Size Distribution and Rupture Hazard on Faults. Bulletin of the Seismological Society of America, 103, 651-674.

Madden, C., Haddad, D.E., Salisbury, J.B., Zielke, O., Arrowsmith, J.R., Weldon, R.J.II, Colunga, J., 2013. Compilation of Slip-in-the-Last Event Data and Analysis of Last Event, Repeated Slip, and Average Displacement for Recent and Prehistoric Ruptures (UCERF3, Appendix R). U.S. Geological Survey Open-File Report 2013–1165-R, California Geological Survey Special Report 228-R, and Southern California Earthquake Center Publication 1792-R.

Mitra, Shankar and Debapriya Paul, 2011. Structural geometry and evolution of releasing and restraining bends: Insights from laser-scanned experimental models. AAPG Bulletin, 95, 1147-1180.

Scharer, K.M., Fumal, T.E., Weldon, R.J., II, Streig, A.R., 2015, Photomosaics and event evidence from the Frazier Mountain paleoseismic site, trench 1, cuts 5–24, San Andreas Fault Zone, southern California (2010–2012): U.S. Geological Survey Open-File Report 2015–1147, 25 p., 3 sheets, http://dx.doi.org/10.3133/ofr20151147.

Scharer, K.M., Fumal, T.E., Weldon, R.J., Streig, A.R., 2014a. Photomosaics and event evidence from the Frazier Mountain paleoseismic site, Trench 1, Cuts 1–4, San Andreas Fault Zone, Southern California (2007-2009), U.S. Geological Survey Open-File Report 2014-1002, 4 sheets, various scales, pamphlet 23 p., http://pubs.usgs.gov/of/2014/1002/.

Scharer, K., Weldon, R., Streig, A., Fumal, T., 2014b. Paleoearthquakes at Frazier Mountain, California delimit extent and frequency of past San Andreas Fault ruptures along 1857 trace, Geophysical Research Letters, v. 41, p. 4527-4534.

Sieh, K.E., 1978. Prehistoric large earthquakes produced by slip on the San Andreas Fault at Pallett Creek, California. Journal of Geophysical Research, 83, 3907-3938.

Streig, A.R., 2014. High Resolution Timing and Style of Coseismic Deformation: Paleoseismic Studies on the Northern and Southern San Andreas Fault (Doctoral Dissertation), Retrieved from https://scholarsbank.uoregon.edu/xmlui/handle/1794/18379

Zilke, O., Arrowsmith, R., Grant Ludwig, L., and Akciz, O., 2012, High-Resolution Topography-Derived Offests along the 1857 Fort Tejon Earthquake Rupture Trace, San Andreas Fault. Bulletin of the Seismological Society of America,102, 1135-1154.